INSTITUTE OF PHYSICS PUBLISHING JOURNAL OF PHYSICS B: ATOMIC, MOLECULAR AND OPTICAL PHYSICS

J. Phys. B: At. Mol. Opt. Phys. **35** (2002) 4759–4771 PII: S0953-4075(02)36573-8

The effects of the Lorentz force on harmonic generation during a laser interaction with a solid target in the nonrelativistic regime

Tingjun Yang and Ji Chen[1]

Chinese Center of Advanced Science and Technology (World Laboratory), PO Box 8730, Bejing 100080, People's Republic of China
and
Department of Modern Physics, University of Science and Technology of China, Hefei 230026, People's Republic of China[2]

E-mail: jichen@ustc.edu.cn

Received 2 May 2002, in final form 14 October 2002
Published 12 November 2002
Online at stacks.iop.org/JPhysB/35/4759

Abstract

In this paper, we use the 'surface currents' model and the nonrelativistic equation of motion of the particle to investigate the harmonic features in the nonrelativistic intensity regime. We also make great efforts to study the effect of Lorentz force in this regime. Our results show that, generally speaking, the Lorentz force effects are quite small. However, in some particular cases, such as the generation of high-order harmonics and large incident angle, the Lorentz force effects are not negligible.

1. Introduction

There has been continued interest in the generation of harmonics from solid targets using ultrashort-pulse lasers during the past 20 years. Many theoretical and experimental studies [1–18] have been reported. At relativistic intensities, i.e. $I\lambda^2$ exceeding 10^{18} W cm^{-2} μm^2 (I is the laser intensity, λ is the laser wavelength), very high order harmonics were observed in many experiments [1–3]. One of the most impressive experiments was performed by Norreys *et al* [2]. In this experiment, harmonics up to 68th were observed at an intensity of $I\lambda^2 = 10^{19}$ W cm^{-2} μm^2. A number of features in the measured spectra were in good agreement with the results from the one-dimensional (1D) particle-in-cell (PIC) simulations of Gibbon [4]. Several theoretical models for the relativistic intensity regime were also proposed to investigate the generation of harmonics in reflection from solid targets. Lichters *et al* [5] developed a 'moving mirror' model which could qualitatively explain the mechanism of the

[1] Author to whom any correspondence should be addressed.
[2] Address for correspondence.

0953-4075/02/234759+13$30.00

harmonic generation for arbitrary incident angles and polarization. In this model, harmonic generation was interpreted as an anharmonic distortion of the laser field upon reflection from a rapidly oscillating surface of the solid target. For small incident angles, Lichters *et al* found excellent agreement with PIC simulations after adjusting the maximum oscillation. For large angles, agreement was not as good. Recently, we extended the 'relativistic surface currents' model [6, 7] to investigate the harmonic generation during the interaction of a p-polarized obliquely incident ultrashort-pulse ultra-intense laser with solid targets. We found that up to 70th harmonics were generated with conversion efficiencies exceeding 10^{-6} which was very close to the result from Norreys *et al*'s experiment and Gibbon's PIC simulations.

When $I\lambda^2 \leqslant 10^{16}$ W cm^{-2} μm^2, the processes involved in the harmonic generation have nonrelativistic characteristics. We call this regime the nonrelativistic regime. Many experiments have been reported in this regime [8, 11–15]. All these experiments showed that there were some different features of harmonics in this regime. First of all, only low-order harmonics can be observed in these experiments. Secondly, all the harmonics prefer to propagate into the specular reflection direction [8, 14, 15]. Thirdly, the harmonic conversion efficiencies depend on the laser polarization. Furthermore, a recent experiment [8] showed that the nth-harmonic intensity can be represented by a power law of the $I_n \propto {I_\omega}^\beta$, where β is called the intensity scaling exponent, and found that for an obliquely incident p-polarized laser beam, second, third and fourth harmonics had intensity scaling exponents of 1.5, 1.8 and 3.8 respectively.

In order to explore the physical mechanism of the harmonic generation and explain the experimental results for the processes in the nonrelativistic intensity regime, in this paper, we use the 'surface currents' model and the nonrelativistic equation of motion of the particle to investigate the harmonic features in the nonrelativistic regime. We focus our discussion on the effects of the Lorentz force and demonstrate that the Lorentz force influences the results of the harmonic generation such as the conversion efficiency and the optimum angle. We also discuss the cases where the 'Lorentz force' effect might be significant. Finally, some other possible effects that might improve the theoretical results are discussed.

2. The 'surface currents' model

Ultrashort, ultra-intense laser pulses focused in gases or on solids can rapidly ionize the targeted medium and plasmas are thereby produced. In underdense plasmas, where the electron density n_e is below the critical density n_c for an electromagnetic wave with frequency ω_0 (where $n_c = \frac{m_e\omega_0^2 c^2}{4\pi e^2}$), the efficiency of the harmonic generation is reduced by the collective fluid response to the particle orbits, and by dephasing of the harmonics relative to the pump [18]. In the opposite case where the solid density plasma (overdense plasma) is produced with $n_e \gg n_c$, the incident laser is almost totally reflected from the vacuum–plasma interface. Harmonics can be generated in the reflected light by the nonlinear mixing of transverse and longitudinal oscillations near the critical surface. Therefore, an effective surface current model can be constructed here.

We assume the vacuum–plasma interface as an ideal conductor. Then a surface current and a surface charge, which act as the sources for harmonics, can be obtained from the boundary conditions of the vacuum–ideal conductor interface that can be written as

$$\vec{n} \cdot \vec{E} = 4\pi\sigma_s \tag{1}$$

$$\vec{n} \times \vec{H} = \frac{4\pi}{c}\vec{j}_s \tag{2}$$

where $\vec{n}$ is the unit vector of the normal direction directed from the plasma to the vacuum, and $\vec{E}$ and $\vec{H}$ are the total electric and magnetic fields (both incident and reflected laser beams

are included) at the side of vacuum, respectively. For a p-polarized obliquely incident laser, they are

$$\vec{H} = -2E_0 \exp[\mathrm{i}(k_x x + k_z z - \omega t)]\vec{e}_y \tag{3}$$

$$\vec{E} = 2E_0 \exp[\mathrm{i}(k_x x + k_z z - \omega t)] \sin\alpha \vec{e}_z \tag{4}$$

where α is the incident angle. For convenience, we adopt the plane wave and replace $\vec{j}_s$ and σ_s with two effective currents $\vec{j}_1$ and $\vec{j}_2$ respectively. The surface current can be written as a bulk current through the delta function $\delta(z)$:

$$\vec{j}_1 = \vec{j}_s \delta(z) \tag{5}$$

and since the surface charge varies with time t, it will contribute an effective current $\vec{j}_2$ due to the equation of continuity:

$$\nabla \cdot \vec{j}_2 + \frac{\partial}{\partial t}\sigma_s \delta(z) = 0 \tag{6}$$

or

$$\vec{j}_2 \cdot \vec{n} = \frac{\partial}{\partial t}\sigma_s. \tag{7}$$

We also assume uniform irradiance within the focal spot, whose radius a is much larger than the laser wavelength. Thus, we have $\vec{j}(\vec{x}, t) = \vec{j}(x, t)$. Finally, we can obtain

$$\vec{j}_1 = \frac{c}{2\pi} E_0 \exp[\mathrm{i}(k_x x - \omega t)]\delta(z)\vec{e}_x \tag{8}$$

$$\vec{j}_2 = \frac{\mathrm{i}\omega}{2\pi} E_0 \exp[\mathrm{i}(k_x x - \omega t)] \sin\alpha \vec{e}_z. \tag{9}$$

The generation of harmonics can be understood in terms of the nonlinear mixing of these two currents.

The 'surface currents' model was first proposed by Wei Yu *et al* [6] in order to investigate the harmonic generation for a normally incident ultrashort-pulse ultra-intense laser. It is helpful to recall its main ideas. In this model, the radiated power per unit solid angle of the nth harmonic from a current source $\vec{j}$ consisting of, say, electrons moving relativistically in the laser field, can be expressed in general as

$$\frac{\mathrm{d}P_n}{\mathrm{d}\Omega} = \frac{n^2\omega_0^2}{(2\pi c)^3}\left|\int \mathrm{d}^3x \int_0^{2\pi} \mathrm{d}\tau \vec{v} \times (\vec{v} \times \vec{j}) \exp[\mathrm{i}n(\tau - k_0 \vec{v} \cdot (\vec{\Delta} + \vec{x}))]\right|^2 \tag{10}$$

where $\vec{j}$ is the surface current, $\vec{v} = (1, \theta, \varphi)$ is the observation direction and $\tau = \omega_0 t$, $\vec{x}$ is the coordinate vector of the source at $\tau = 0$. The $\vec{\Delta}$ is its displacement and can be written as $\vec{\Delta} = \int_0^{\omega t} \vec{v}(\vec{x}, \tau')\,\mathrm{d}\tau'$, where $\vec{v}$ is the single-electron quiver velocity in the incident laser field. Therefore $\vec{x} + \vec{\Delta}$ is the instantaneous location of the source. Compared with some previous models [9, 10], this model takes into account the coordinate vector of the current source as well as its displacement in the exponent phase factor which, as we will show later, contributes a factor that can determine the directionality of the harmonics.

$\vec{v}$ can be derived from the equation of motion of the electron in the electromagnetic field. Because we investigate the nonrelativistic intensity regime, we can make some approximation. Since $v/c \ll 1$ is satisfied in this regime, we can treat the Lorentz force $\vec{F}_{Lor} = -\frac{e}{c}\vec{v} \times \vec{B}$ as a perturbation and expand the displacement of the current source to the order of q^2

$$\vec{\Delta} = \frac{q}{k}\cos(k_x x - \omega t)(-\cos\alpha \vec{e}_x + \sin\alpha \vec{e}_z) + \frac{q^2}{8k}\sin 2(k_x x - \omega t)(\sin\alpha \vec{e}_x + \cos\alpha \vec{e}_z) \tag{11}$$

where $q = \frac{eE_0}{m\omega c} = 0.85 \times 10^{-9}\sqrt{I\lambda^2}$ is the laser strength parameter ($I = \frac{cE_0^2}{8\pi}$ is in units of W cm^{-2}, λ is in units of μm).

In the cylindrical coordinate system, equation (10) can be expressed as

$$\frac{\mathrm{d}P_n}{\mathrm{d}\Omega} = \frac{n^2\omega_0^2}{(2\pi c)^3}\left|\int_0^a \rho\,\mathrm{d}\rho \int_0^{2\pi} \mathrm{d}\phi\ \exp[-\mathrm{i}nk\rho\sin\theta\cos(\phi-\varphi)] \int_0^{\varepsilon} \mathrm{d}z\ \exp[-\mathrm{i}nk\cos\theta z]\right.$$
$$\left.\times \int_0^{2\pi} \mathrm{d}\tau\ \vec{\nu}\times(\vec{\nu}\times\vec{j})\exp[\mathrm{i}n(\tau - k\vec{\nu}\cdot\vec{\Delta})]\right|^2 \tag{12}$$

where a is the focal radius of the laser beam. Therefore, we can solve the integral in equation (12) to yield

$$\frac{\mathrm{d}P_n}{\mathrm{d}\Omega} = \frac{ca^2E_0^2}{2\pi}\left[\frac{J_1(nka\xi)}{\xi}\right]^2 Y_n\left[\cos^2\theta + \sin^2\theta\sin^2\varphi\right.$$
$$\left. + 4\sin^2\left(\frac{1}{2}nk\cos\theta\varepsilon\right)\left(\frac{1}{n^2}\sin^2\alpha\tan^2\theta - \frac{1}{n}\sin\alpha\sin\theta\cos\varphi\right)\right] \tag{13}$$

where

$$Y_n = \left|\frac{1}{2\pi}\int_0^{2\pi}\mathrm{d}\tau\ \exp[\mathrm{i}(n-1)\tau + \mathrm{i}nQ\cos\tau + \mathrm{i}nQ'\sin 2\tau\right|^2$$
$$= \left|\sum_{\mu+2\upsilon=1-n}\mathrm{i}^{\mu}J_{\mu}(nQ)J_{\upsilon}(nQ')\right|^2 = \left|\sum_{\mu+2\nu=n-1}J_{\mu}(nQ)J_{\nu}(nQ')\right|^2 \tag{14}$$

$$\xi = (\sin^2\theta + \sin^2\alpha - 2\sin\theta\sin\alpha\cos\varphi)^{1/2} \tag{15}$$

$$Q = q(\sin\theta\cos\varphi\cos\alpha - \cos\theta\sin\alpha) \tag{16}$$

$$Q' = \frac{q^2}{8}(\sin\alpha\sin\theta\cos\varphi + \cos\theta\cos\varphi). \tag{17}$$

We know that the electromagnetic wave can only propagate into a layer near the surface of the metal, which is called the conductor skin effect. Here ε denotes the depth of the layer and we can estimate it with the skin depth, which can be expressed as $\delta = \frac{c}{\sqrt{2\pi\mu\omega\sigma}}$ [20]. We figure out that δ is several nanometres, thus $k\varepsilon \ll 1$ is satisfied in the experiments we investigate. Therefore, we can neglect the last term in the square brackets of equation (13) for the low-order harmonics. We can then rewrite equation (13) as

$$\frac{\mathrm{d}P_n}{\mathrm{d}\Omega} = \frac{ca^2E_0^2}{2\pi}\left[\frac{J_1(nka\xi)}{\xi}\right]^2 Y_n(\cos^2\theta + \sin^2\theta\sin^2\varphi). \tag{18}$$

Harmonic emission can also be considered as nonlinear scattering of light and the scattering efficiency of the nth harmonic can thereby be expressed as follows [6]:

$$\eta_n = \frac{3c\sigma_T}{2\pi\mathrm{e}^2\omega^2a^2q^2}\int\frac{\mathrm{d}P_n}{\mathrm{d}\Omega}\,\mathrm{d}\Omega \tag{19}$$

where σ_T is the Thompson cross section.

3. Some results

First of all we consider the angular distribution of the harmonic radiation. Instead of making the assumption of a point-like interaction region as in many previous works [9, 10], in this model we take into account the finite size of the focal spot, which will contribute a factor $[\frac{J_1(nka\xi)}{\xi}]^2$ in our expression. The factor has often appeared in optics in connection to diffraction from a circular hole. For $ka \gg 1$, we can see that $[\frac{J_1(nka\xi)}{\xi}]^2$ peaks sharply at $\xi = 0$ and falls rapidly

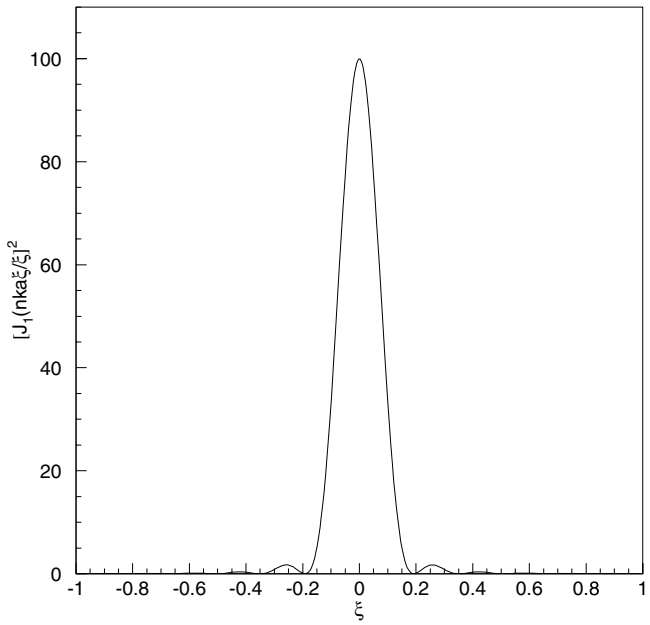

Figure 1. The variation of factor $[\frac{J_1(nka\xi)}{\xi}]^2$ for $n = 2$ and $ka = 10$.

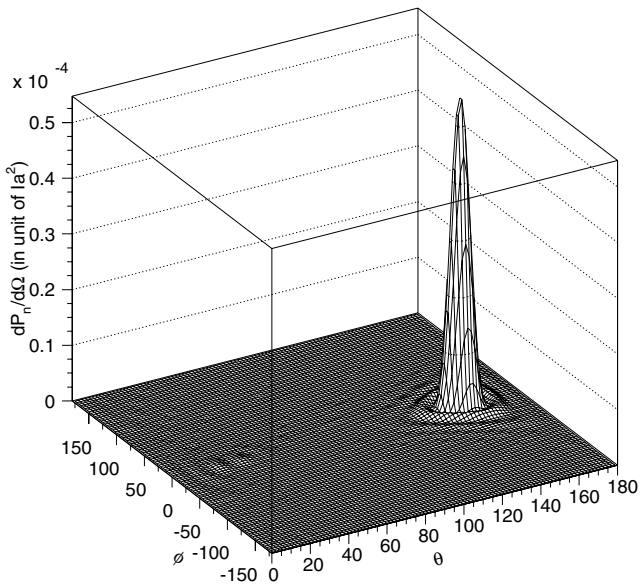

Figure 2. The angular distribution of harmonics for $q = 0.001$. The value of $\frac{dP_n}{d\Omega}$ has been divided by the factor Ia^2; other parameters are the same as in figure 1.

to zero at other values, as is shown in figure 1 for $n = 2$ and $ka = 10$. In the region that can be observed ($\theta \in [\frac{\pi}{2}, \pi], \varphi \in [0, 2\pi)$), ξ can take the value of zero only when $\theta = \pi - \alpha$ and $\varphi = 0$, which just represents the specular reflection direction. So we have demonstrated that the harmonic radiation occurs predominantly in the specular direction. We can also see clearly that $\frac{dP_n}{d\Omega}$ peaks at $\theta = \pi - \theta$ and $\varphi = 0$ for $n = 2$ and $ka = 10$ in figure 2. In the real

experiments, ka will achieve a much higher value (about 100), which means that the peak will be sharper than is shown in figure 2. We conclude that the interaction of a shorter-wavelength laser with solid targets can produce more directional harmonic radiation.

Since almost all the energy of the harmonics is focused into the direction of specular reflection, for convenience we can substitute the differential value of the conversion efficiency in the direction of specular reflection for the integral form (19). A coefficient of proportionality is required in order to estimate the conversion efficiency. Using the similar method described by Ganeev *et al* [8], we obtain the conversion efficiency in a small solid angle $\Delta\Omega$ as

$$\eta_n = 4\Delta\Omega\left[\frac{J_1(nka\xi)}{\xi}\right]^2 Y_n(\cos^2\theta + \sin^2\theta\sin^2\varphi) \tag{20}$$

where $\Delta\Omega = \frac{a^2}{r^2}$. a is the focus radius of the incident laser and r is the distance between incident spot on the solid surface and the spectrometer. In order to obtain the intensity scaling exponent for the conversion efficiency of the harmonic generation, we need to discuss Y_n in (14) more carefully. Usually the numerical method must be used in order to obtain an accurate value of Y_n. However, in the case of the nonrelativistic intensity regime, we can easily find that $q \ll 1$ and $nq, nq^2 \ll 1$ for the low-order harmonics are satisfied. From the feature of the Bessel function we know that terms with μ or υ of high absolute value in (14) can be neglected. Therefore, we can obtain $Y_2 = J_1^2(2Q)J_0^2(2Q')$, $Y_3 = |J_2(3Q)J_0(3Q') + J_0(3Q)J_1(3Q')|^2$ and $Y_4 = |J_3(4Q)J_0(4Q') + J_1(4Q)J_1(4Q')|^2$, for example. For $x \ll 1$, $J_n(x)$ is proportional to x^n, thus we find that the efficiency η_n is proportional to $q^{2(n-1)}$ and is also proportional to I^{n-1}. Therefore we get intensity scaling exponents of 1–3 for second, third and fourth harmonics, respectively. Ganeev *et al*'s experiment showed intensity scaling exponents of 1.5, 1.8, and 3.8 respectively. The discrepancies of our theoretical results and the experiments are negligible for the third harmonic, but cannot be neglected for the second and fourth harmonics. However, as we check Ganeev *et al*'s [8] experimental results in the figures 2–4, we find that deviations of experimental spots from the fitting lines are quite large for the second and fourth harmonics, which can contribute a lot to the discrepancies of the experiment and our theory. The result also implies that the high-intensity laser has to be used in order to enhance the efficiencies of harmonic generation and obtain high-order harmonics.

Figure 3 shows the conversion efficiency of harmonic generation versus the harmonic number for $I = 10^{15}$ W cm^{-2}, $\lambda = 1.053$ μm and $\alpha = 67.5°$ which are the same as in Ganeev *et al*'s [8] experiment. It can be seen that our results are quite close to the data of Ganeev's experiment, except for the fourth harmonic.

Now we investigate the influence of incident angle of the laser on the harmonic emission. Figure 4 shows the conversion efficiency of second harmonics versus the incident angle for $I = 10^{15}$ W cm^{-2}, $\lambda = 1.053$ μm. The peak conversion occurs for an incident angle of 34.7°.

Finally, let us discuss the influence of the intensity of the incident laser on the harmonic emission. Conversion efficiency versus harmonic number for different values of q is shown in figure 5. We can see that the conversion efficiency falls rapidly as harmonic number increases for $q \ll 1$ which just represents the nonrelativistic intensity regime. For $q \sim 1$, efficiency falls more slowly. This demonstrates that the ultra-intense laser is indispensable in order to obtain high-order harmonics.

4. The effect of Lorentz force in the nonrelativistic intensity regime

We now discuss the effects of Lorentz force in the nonrelativistic intensity regime. The Lorentz force is the main cause of nonlinearity of the orbit of a single electron in an electromagnetic plane-wave. In previous works, it is sometimes suggested that the Lorentz force can be

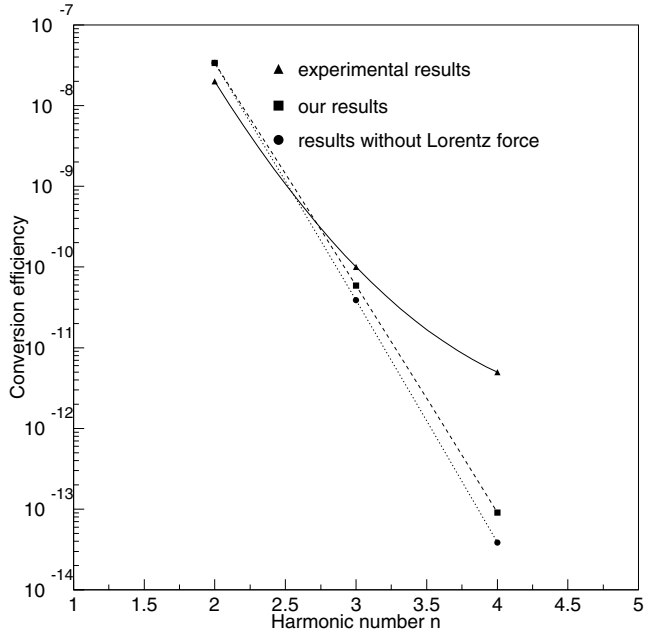

Figure 3. Conversion efficiency versus the harmonic number for $I = 10^{15}$ W cm^{-2}, $\lambda = 1.053\,\mu$m and $\alpha = 67.5°$ with $\Delta\Omega = 3.0 \times 10^{-9}$. Triangles: experimental results [8]. Squares: results with consideration of Lorentz force. Circles: results without consideration of Lorentz force.

neglected in the nonrelativistic regime due to the small factor $\frac{v}{c}$. The electron will make the harmonic oscillation in the direction of electric field of the electromagnetic wave if we do not take into account the Lorentz force.

In (11), though it was from the first perturbation of the Lorentz force term, the orbit property of a single electron is kept. In order to show this result, let us rewrite (11) as

$$\vec{r} = \frac{q}{k}\cos(k_x x - \omega t)(-\cos\alpha\vec{e_x} + \sin\alpha\vec{e_z}) + \frac{q^2}{8k}\sin 2(k_x x - \omega t)(\sin\alpha\vec{e_x} + \cos\alpha\vec{e_z}). \tag{21}$$

In the coordinate system where $\vec{e'_x} = \sin\alpha\vec{e_x} + \cos\alpha\vec{e_z}$, $\vec{e'_y} = -\cos\alpha\vec{e_x} + \sin\alpha\vec{e_z}$, the orbit can be written as

$$16k^2x'^2 = k^2y'^2(q^2 - k^2y'^2). \tag{22}$$

The orbits of a single electron in the electromagnetic field of linearly polarized light are depicted graphically in figure 6. The well known figure-of-eight was obtained as the same result in many previous works (the definition of q may have a different factor) [9, 10].

When we checked the expression of Y_n in (14), we found that though the term containing Q' (the modification after taking into account Lorentz force) is smaller than the term containing Q in the nonrelativistic intensity regime, it might influence the final results since it contributes an exponent factor in the integral of (14). In order to show the importance of the Lorentz force in the high-harmonics generation, we give some numerical results.

Figure 7 shows the ratio η_n^L/η_n^{noL} versus harmonic number. All the parameters are the same as in Ganeev *et al*'s experiment [8]. The difference between the two results can be neglected only for the second harmonic. As the harmonic number increases, the difference becomes larger. We can conclude that the Lorentz force plays an important role, especially in the generation of high-order harmonics, even in the nonrelativistic regime.

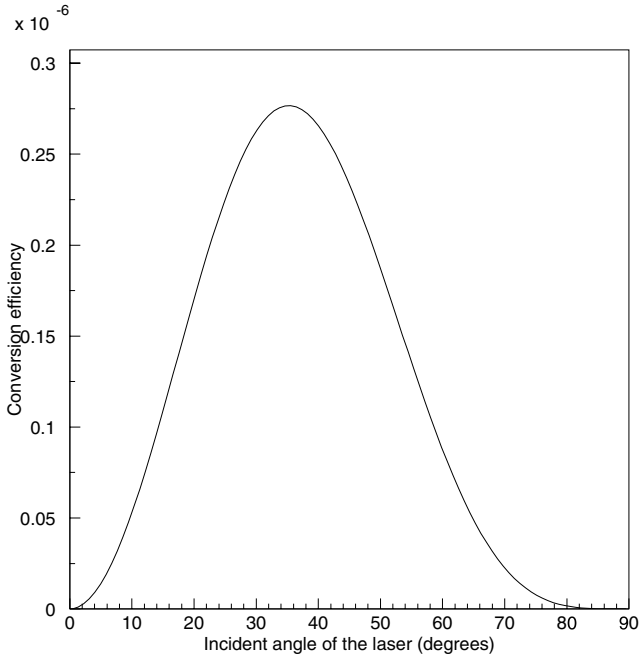

Figure 4. Conversion efficiency versus the incidence angle for the second harmonics; other parameters are the same as Ganeev's [8].

Now we demonstrate that the ratio η_n^L/η_n^{noL} has no dependency on the intensity of the incident laser in the nonrelativistic regime. As we discuss above, the efficiency η_n^L is proportional to $q^{2(n-1)}$ and is also proportional to I^{n-1}. When we neglect the effect of Lorentz force, the expression of Y_n changes into $J_{n-1}^2(nQ)$, which means that the efficiency η_n^{noL} is also proportional to $q^{2(n-1)}$ and I^{n-1}. Therefore the ratio will remain constant in a very wide nonrelativistic intensity regime.

Figure 8 shows the ratio η_n^L/η_n^{noL} versus incident angle α for the second, third and fourth harmonics. The Lorentz force effect can be neglected only for the second harmonics and becomes more obvious for higher-order harmonics. For harmonic number equal to or larger than 3, and especially for large incident angle, the Lorentz force plays an important role in the generation of harmonics. We can see from figure 8 that the ratio becomes 1 when the incident angle α is 45°, which means the Lorentz force has no influence on the harmonic emission for this angle. This result can be obtained from the expression of Q' in (14). In the specular direction, $Q' = -\frac{q^2}{8}\cos(2\alpha)$. For $\alpha = 45°$, $Q' = 0$. Therefore the Lorentz force has no effect on the harmonic generation. For $\alpha > 45°$, $Q' > 0$ and for $\alpha < 45°$, $Q' < 0$. From the expression of Y_n, we find that positive Q' can increase the conversion efficiency while negative Q' can decrease the conversion.

Finally, in order to investigate the influence of Lorentz force on the optimum incident angle, we show the conversion efficiency versus the incident angle α for the third and fourth harmonics in figures 9 and 10. For the third harmonics, the conversion efficiency peaks at 40.6° (not 39.2°) after taking into account the Lorenz force. For the fourth harmonics, the conversion efficiency peaks at 45.1° (not 40.6°). The discrepancy is obvious for high-order harmonics. This result may provide a practical method to test the Lorentz force effect in the nonrelativistic regime.

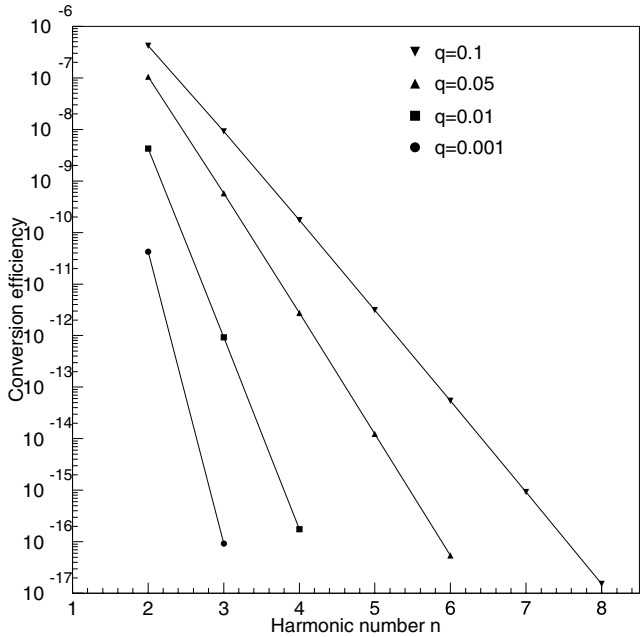

Figure 5. Conversion efficiency versus harmonic number for q of different values; other parameters are the same as Ganeev's [8].

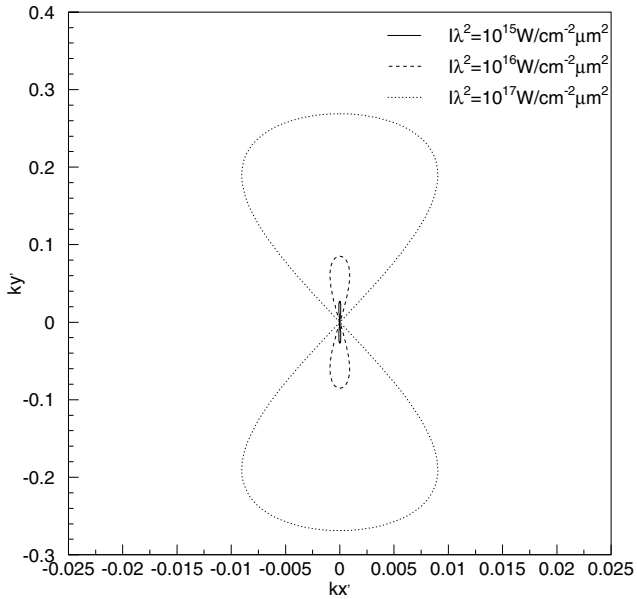

Figure 6. Characteristic orbits of free electrons in a plane electromagnetic wave. The trajectories correspond to the laser strength parameter of 10^{15} (solid curve), 10^{16} (dashed curve), 10^{17} (dotted curve), respectively.

5. Further discussion and summary

In this paper, we have concentrated on the effects of the Lorentz force on harmonic generation. In doing so, we have omitted a variety of other physical processes which are equally important

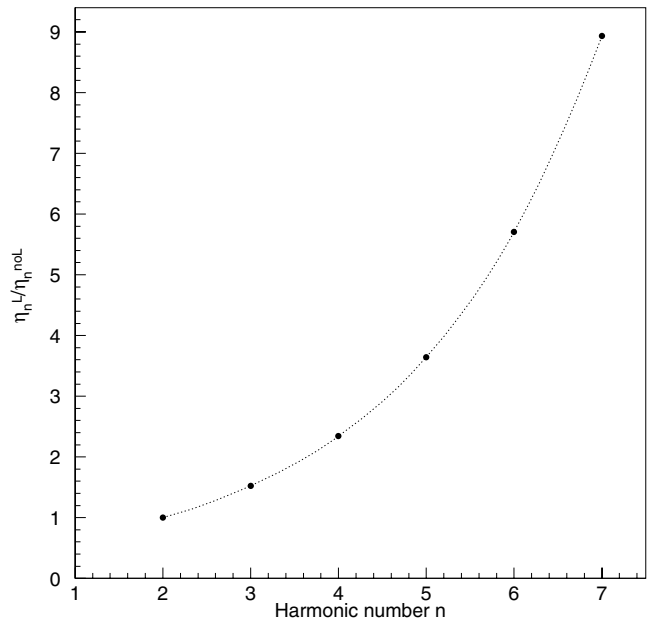

Figure 7. The ratio η_n^L/η_n^{noL} versus harmonic number; all the parameters are the same as Ganeev's [8].

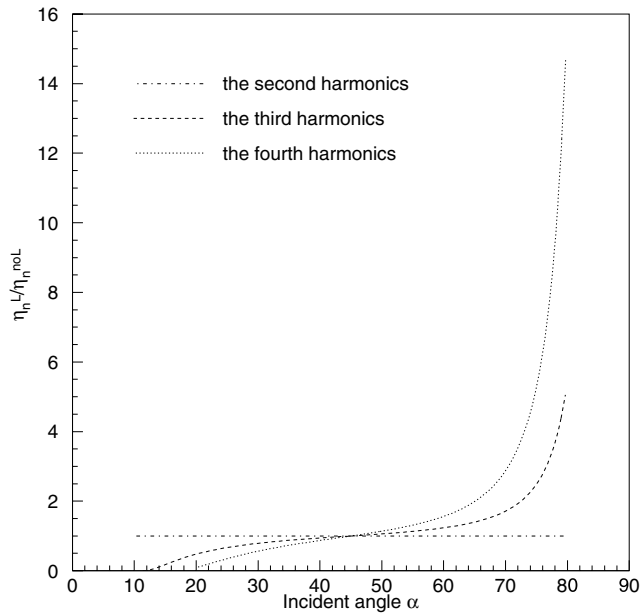

Figure 8. The ratio η_n^L/η_n^{noL} versus incident angle α; other parameters are the same as Ganeev's [8].

in the generation of harmonics. It is often suggested that the harmonics are generated from the harmonic content of the electron density n_e and the nonlinear orbit of the single electron in a

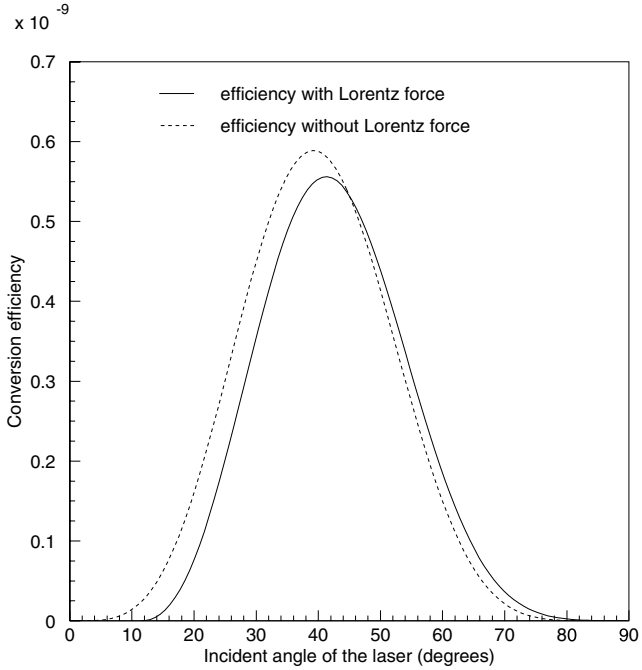

Figure 9. Conversion efficiency versus the incidence angle for the third harmonics; other parameters are the same as Ganeev's [8]; solid curve: efficiency with Lorentz force, dashed curve: efficiency without Lorentz force.

strong electromagnetic plane-wave. In our model, the latter was included using a perturbation expansion of the displacement. However, the details of the electron density distribution were neglected, which might be responsible for the discrepancies displayed in figure 3, for harmonic number equal to or larger than 4. A detailed discussion concerning this effect can be found in [19], which gives a nonlinear current $j_{2\omega}$ at the second-harmonic frequency

$$j_{2\omega} \propto \left[\frac{\omega_p^2}{4\omega_0^2} \nabla(\boldsymbol{E} \cdot \boldsymbol{E}) + \frac{\omega_p^2}{\omega_0^2 - \omega_p^2} (\boldsymbol{E} \cdot \nabla \ln n_e) \boldsymbol{E} \right] \tag{23}$$

where $\omega_p = (4\pi n_e e/m)^{1/2}$ is the plasma resonance frequency. This current should act as a source for the harmonic generation.

In conclusion, in this paper we use the 'surface currents' model and expand the electron displacement in power series and calculate the differential scattering cross-sections for the harmonics. Our results show that harmonic generation occurs preferentially in the specular direction. We find an intensity scaling exponent of $n - 1$ for the nth harmonics. We also estimate the conversion efficiencies and make some comparisons with data of the experiments by Ganeev *et al*. Almost all these results are in good agreement with the experiments. Though our discussion has focused on the nonrelativistic regime, our results imply that the ultra-intense and short-wavelength laser is indispensable in order to obtain high-order and highly directional harmonics.

We also study the effect of Lorentz force in the nonrelativistic regime. We obtain the orbit of a single electron in strong electromagnetic plane-wave (figure-of-eight) in a more straightforward and simpler way. We explore many factors that might influence the effect of

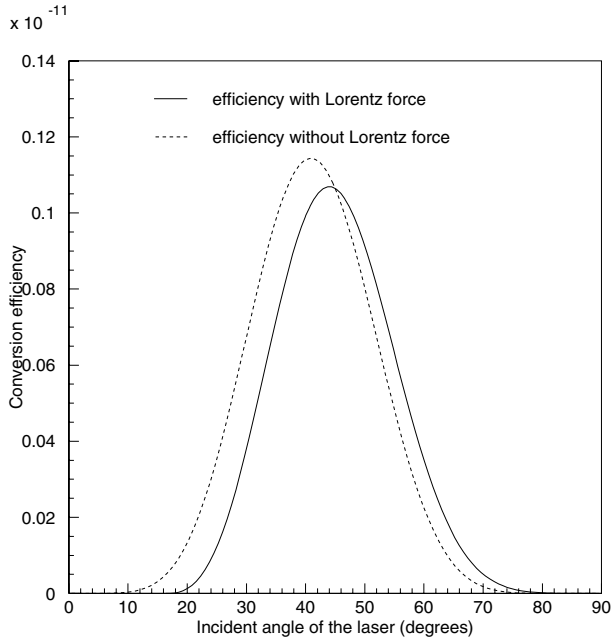

Figure 10. Conversion efficiency versus incidence angle for the fourth harmonics; other parameters are the same as Ganeev's [8]; solid curve: efficiency with Lorentz force, dashed curve: efficiency without Lorentz force.

Lorentz force such as the harmonic number, the laser intensity and the incident angle. Our results show that, generally speaking, the Lorentz force effects are negligibly small. However, in some particular cases, such as the generation of high-order harmonics and the large incident angle, the Lorentz force effects are not negligible.

Acknowledgment

This work was supported by the National Natural Science Foundation of China under grant numbers 10075043 and 10074060.

References

[1] Chambers D M *et al* 1998 *Opt. Commun.* **148** 289
[2] Norreys P A *et al* 1996 *Phys. Rev. Lett.* **76** 1832
[3] Tarasevitch *et al* 2000 *Phys. Rev.* A **62** 023816
[4] Gibbon P 1996 *Phys. Rev. Lett.* **76** 50
[5] Lichters R *et al* 1996 *Phys. Plasmas* **3** 3425
[6] Yu W *et al* 1998 *Phys. Rev.* E **57** R2531
[7] Wu S *et al* 2001 *Phys. Lett.* A **286** 282
[8] Ganeev R A *et al* 2001 *Phys. Rev.* E **63** 026402
[9] Gibbon P 1997 *IEEE J. Quantum Electron.* **33** 1915
[10] Sarachik E S and Schappert G T 1970 *Phys. Rev.* D **1** 2738
[11] Foldes I B *et al* 2000 *Laser Phys.* **10** 264
[12] Carman R L *et al* 1981 *Phys. Rev.* A **24** 2649
[13] Besserides B *et al* 1982 *Phys. Rev. Lett.* **49** 202
[14] Marjoribanks R S *et al* 1996 *Bull. Am. Phys. Soc.* **41** 1424

[15] Ishizawa A *et al* 1999 *IEEE J. Quantum Electron.* **35** 60
[16] Linde D von der *et al* 1995 *Phys. Rev.* A **52** R52
[17] Wilks S C *et al* 1993 *IEEE Trans. Plasma Sci.* **21** 120
[18] Esarey E *et al* 1993 *IEEE Trans. Plasma Sci.* **21** 95
[19] Shen R Y 1984 *The Principles of Nonlinear Optics* (New York: Wiley) p 553
[20] Jackson J D 1975 *Classical Electrodynamics* (New York: Wiley)